文章编号：1001－9014(2016)01－0001－06

DOI:10.11972/j.issn.1001－9014.2016.01.001

Composition-dependent optical properties of plasmonic $Ag_x In_{1-x}$ alloys

YANG Shang-Dong, ZHENG Yu-Xiang*, ZHANG Dong-Xu, ZHANG Jin-Bo, HU Er-Tao, ZHANG Rong-Jun, WANG Song-You, CHEN Liang-Yao

(Department of Optical Science and Engineering, and Shanghai Ultra-Precision Optical Manufacturing Engineering Center, Fudan University, Shanghai 200433, China)

Abstract: Five samples of Ag-In alloy films with different compositions were deposited on Si substrates by magnetron sputtering. The optical properties of these films were studied by spectroscopic ellipsometry. The dielectric functions of the alloy films significantly increase as the In concentration in the Ag-In alloy films is increased. For Ag-based alloys, a typical interband transition occurs near 3.9 eV. In the tested alloy films, however, this transition energy exhibits a blue shift with increasing In concentration. The optical properties of the alloy films were found to be tunable by varying their In concentrations. The values of the Quality (Q) factors of the $Ag_{0.93}In_{0.07}$ film are higher than those of other alloy films. At a certain wavelength range, the alloys' Q factors even exceed those of pure Au and Cu. Our results show that Ag-In alloys have significant potential for application in metamaterials and plasmonic devices.

Key words: Ag-In alloy films, optical properties, spectroscopic ellipsometry, magnetron sputtering
PACS: 78.66.Bz, 78.20.Ci, 81.05.Bx, 81.15.Cd

等离子体材料银铟合金光学性质的组分依赖性

杨尚东，郑玉祥*，张冬旭，张金波，胡二涛，张荣君，王松有，陈良尧
（复旦大学 光科学与工程系，上海超精密光学制造工程技术研究中心，上海 200433）

摘要：采用磁控溅射方法在硅衬底上生长了五个不同组分的银铟合金薄膜.采用椭圆偏振光谱仪研究银铟合金薄膜的光学性质.银基金属薄膜一般在3.9 eV附近出现典型的带间跃迁.随着铟含量的增加，银铟合金薄膜的介电函数呈现出明显增加的趋势，典型带间跃迁能量也出现蓝移.结果表明，银铟合金薄膜的光学性质可以通过其中铟元素的含量进行调控.$Ag_{0.93}In_{0.07}$薄膜比其他四种组分的银铟合金薄膜有着更大的品质因子(Q因子)，而且在一些波段甚至比纯金属金和铜的Q因子都要大，这表明银铟合金材料具有成为新型等离子体材料的潜力.

关 键 词：银铟合金薄膜；光学性质；椭圆偏振光谱仪；磁控溅射

中图分类号：O43　　**文献标识码**：A

Introduction

Metamaterials and plasmonic devices have attracted considerable attention of researchers and developers because of their promising applications in invisibility cloaks[1-2], super lenses[3-4], and satellite antennas. Au and Cu, which have an abundance of free electrons, are frequently used as plasmonic materials and metamaterials. However, sizeable metal loss is a major obstacle in plasmonic applications[5-6]. Although optical grain materials have been proposed to reduce the loss of metals, some optical grain materials such as rhodamine 6G (R6G) and rhodamine 800 (Rh800)[7-8] need complicated manufacturing process which cause additional noises[9-10]. Higher densities of free electrons are found in alloys, which can fully realize the potential of plasmonic applications[11]. Considerable efforts have been made to investigate noble metal alloys, including Ag-Au, Ag-Cu, Ag-Al, Ag-Zn, and Ag-Pt[12-13]. However, little has

Received date: 2015-03-12, **revised date**: 2015-05-29　　**收稿日期**：2015-03-12，**修回日期**：2015-05-29
Foundation items: Supported by National Natural Science Foundation of China (61275160, 11374055, 11174058, 60938004), Projects of Science and Technology Commission of Shanghai Municipality (12XD1420600)
Biography: YANG Shang-Dong (1989-), male, Shanghai, master. Research area involves optical properties of solids. E-mail: 12210720005@fudan.edu.cn
* **Corresponding author**: E-mail: yxzheng@fudan.edu.cn

been reported on the optical properties of Ag-In alloy films [14-15].

This study investigated the optical properties of five samples of Ag-In alloy films, which were deposited on Si substrates by magnetron sputtering. The optical properties of these films were examined by spectroscopic ellipsometry (SE). Atomic force microscopy (AFM) was used to observe the surface topography and nanostructure of the films. Energy-dispersive X-ray (EDX) spectroscopy was used to detect the elemental compositions of the Ag-In alloy films. The results confirm that the optical properties of the Ag-In alloy films are sensitive to In concentration, especially at long wavelengths.

1 Experiment

Five samples of Ag-In alloy films, $Ag_{0.55}In_{0.45}$, $Ag_{0.67}In_{0.33}$, $Ag_{0.78}In_{0.22}$, $Ag_{0.87}In_{0.13}$, and $Ag_{0.93}In_{0.07}$, were deposited by magnetron sputtering on n-type Si (100) substrates (purity: 99.99%) at room temperature. The deposition rate was 0.1 nm/s and the deposition time was 1000 s. Before deposition, the Si substrates were cleaned using ethanol, then acetone, and finally deionized water. SE was used to investigate the optical properties of these thin films[16-17]. The ellipsometric parameters were measured in the wavelength range of 275 ~800 nm at three different incident angles of 65°, 70°, and 75°. After selecting an appropriate model to represent the thin-film system, we used the Film Wizard (Scientific Computing International, USA) software program to fit the optical constants of the samples. The surface topographies and nanostructures of the alloy films were observed by AFM (VT1000, Veeco, USA) in the non-contact mode. The compositions of the Ag-In alloy films were determined by EDX (XL30FEG, Philips, The Netherland).

2 Results and discussion

Each element exhibits a unique X-ray spectrum; using these characteristic spectra. The types and ratios of atoms in the samples were determined. The EDX results, shown in Table 1, present the compositions of all samples tested in this study.

Table 1 EDX results of Ag-In alloy films
表1 银铟合金薄膜的X射线能谱仪测量结果

Sample(Ag_xIn_{1-x})	Atom Ratio(x: 1-x)
(a)	100: 0
(b)	55: 45
(c)	67: 33
(d)	78: 22
(e)	87: 13
(f)	93: 7

Figure 1 shows the AFM images of the five Ag-In alloy films as well as that of a pure Ag film, revealing changes in the size of particles at the surfaces of the samples. The grain size is gradually diminished, and the surface roughness r_q decreases from 18.8 to 0.573 nm with decreasing In concentration.

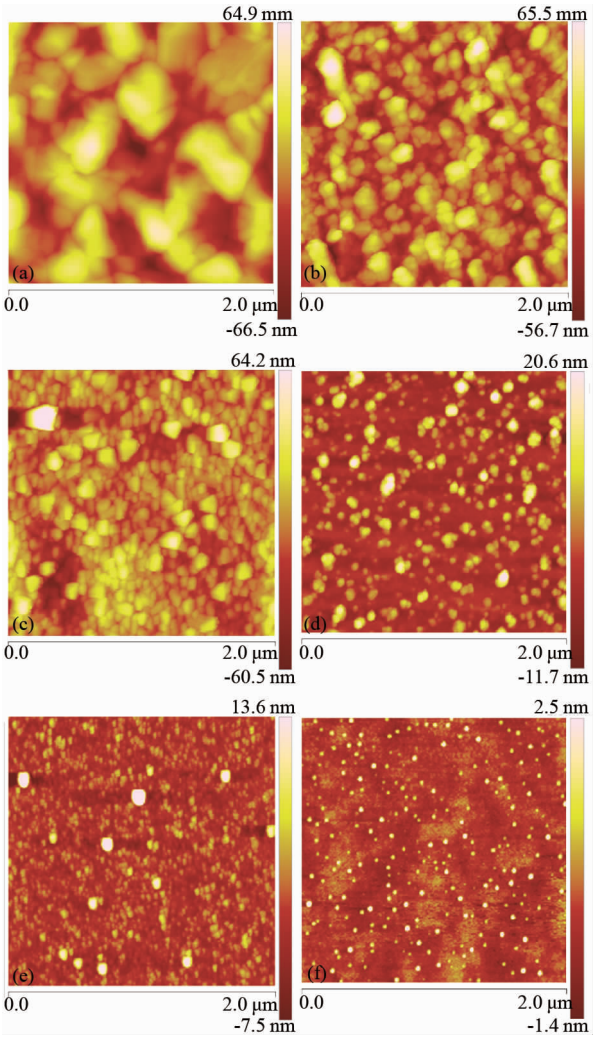

Fig. 1 AFM images of Ag-In alloy films with different concentrations: (a) Ag; (b) $Ag_{0.55}In_{0.45}$; (c) $Ag_{0.67}In_{0.33}$; (d) $Ag_{0.78}In_{0.22}$; (e) $Ag_{0.87}In_{0.13}$; (f) $Ag_{0.93}In_{0.07}$
图1 不同组分银铟合金薄膜的原子力显微镜照片:(a) Ag; (b) $Ag_{0.55}In_{0.45}$; (c) $Ag_{0.67}In_{0.33}$; (d) $Ag_{0.78}In_{0.22}$; (e) $Ag_{0.87}In_{0.13}$; (f) $Ag_{0.93}In_{0.07}$

The optical properties of the Ag-In alloy films were investigated with a rotating polarizer-analyzer ellipsometer (RPAE)[18]. According to the AFM images, a rough surface was formed on each sample, and a four-layer model (air/roughness/Ag-In alloy/Si substrate) of a sample and its environment was used to fit the ellipsometric parameters. An effective-medium-approximation (EMA) model[19-20] was applied to represent the dielectric functions of the roughness layer, which are described by the following equation:

$$\frac{\varepsilon_{\text{roughness}}-1}{\varepsilon_{\text{roughness}}+2}=f\cdot\frac{\varepsilon_{\text{Ag-In}}-1}{\varepsilon_{\text{Ag-In}}+2}, \quad (1)$$

where f is the volume fraction of the Ag-In alloy, $\varepsilon_{\text{roughness}}$ and $\varepsilon_{\text{Ag-In}}$ are the dielectric constants of the rough surface and the Ag-In alloy, respectively, and the dielectric constant of a void is assumed to be 1.

The Drude-Lorentz (DL) model[21] was utilized to

describe the dielectric responses of different component materials according to

$$\varepsilon_{DL} = \varepsilon_\infty - \frac{\omega_p^2}{\omega^2 + i\omega\gamma} + \sum_k \frac{C_k}{\omega_k^2 - \omega(\omega + i\gamma_k)}, \quad (2)$$

where ω_p is the unscreened plasma frequency, γ is the plasmon damping constant of the Drude part, C_k, ω_k and γ_k are the strength parameter, resonant frequency, and damping factor, respectively, of different oscillators. In Eq. 2, the first term is nondispersive and arises from other higher interband transitions, while the second term is related to the intraband transition, and the third term represents the contributions of interband transitions[22-23].

Figure 2 shows the data fitting results of the ellipsometric parameters—the amplitude ratio Ψ and phase shift Δ between the reflected p- and s-polarized light—where the points and lines represent the measured parameters and calculated curves, respectively. All of the fitting parameters are listed in Table 2. It can be clearly seen that the calculated curves agree well with the measured parameters, indicating that the four-layer model used in the above fitting process is reasonable and acceptable.

Table 2　Fitting parameters of Ag-In alloy films
表 2　银铟合金薄膜的椭偏拟合参数

Parameters	Ag	$Ag_{0.55}In_{0.45}$	$Ag_{0.67}In_{0.33}$	$Ag_{0.78}In_{0.22}$	$Ag_{0.87}In_{0.13}$	$Ag_{0.93}In_{0.07}$
d(nm)	108.87	103.59	105.81	102.71	102.90	100.77
ε_∞	5.49	2.82	2.53	3.62	4.48	4.86
E_p(eV)	8.85	7.97	8.19	8.25	8.44	8.71
Γ_p(eV)	34.56	20.91	35.87	43.30	36.56	28.02
C_1(eV^2)	2.91	4.83	1.70	2.72	4.30	3.40
E_1(eV)	1.64	0.02	4.27	3.11	0.01	0.09
Γ_1(eV)	2.43	1.37	1.72	2.98	0.28	0.01
C_2(eV^2)	3.27	3.65	2.96	1.56	2.37	2.76
E_2(eV)	0.01	3.26	3.31	3.85	1.75	1.32
Γ_2(eV)	0.01	3.88	3.50	1.75	2.15	2.06
C_3(eV^2)	1.40	0.65	5.64	1.51	2.53	2.56
E_3(eV)	3.43	4.57	0.01	4.55	3.64	3.58
Γ_3(eV)	2.46	0.40	1.08	0.85	2.56	3.01
C_4(eV^2)	0.94	1.61	0.87	4.70	1.34	1.47
E_4(eV)	4.16	4.37	4.59	0.03	4.51	4.42
Γ_4(eV)	0.33	1.68	0.60	0.60	0.78	0.89

The dielectric functions of the Ag-In alloy films are shown in figure 3. For the Ag-based alloys, a typical interband transition occurs near 3.9 eV and the intraband transition dominates at energies below 3.9 eV. The real (ε_1) and imaginary (ε_2) parts of the dielectric functions both increased with increasing In content in the wavelength range of 320 ~ 800 nm. The value of ε_1 of all samples except pure Ag is negative in the wavelength range of 275 ~ 320 nm. The frequency at $\varepsilon_1 = 0$ is the critical frequency at which the properties of the metal transform from the high-reflectivity mode to the weak-absorption mode. For the Ag-In alloy films, this critical frequency was not observed in the measured wave band. It can be interpreted by that the addition of In changes the alloy's electronic band structure, causing the blue shift of the interband transition, thus resulting in a higher critical frequency and shorter wavelength at $\varepsilon_1 = 0$. As is well known, the imaginary parts of dielectric functions are related to the process of absorption in the films. Owing to the blue shift of interband transitions, the values of ε_2 of the alloy films exhibit absorption peaks at shorter wavelengths than that of pure Ag. As In concentration is increased, ε_2 increases, indicating large damping and great energy loss.

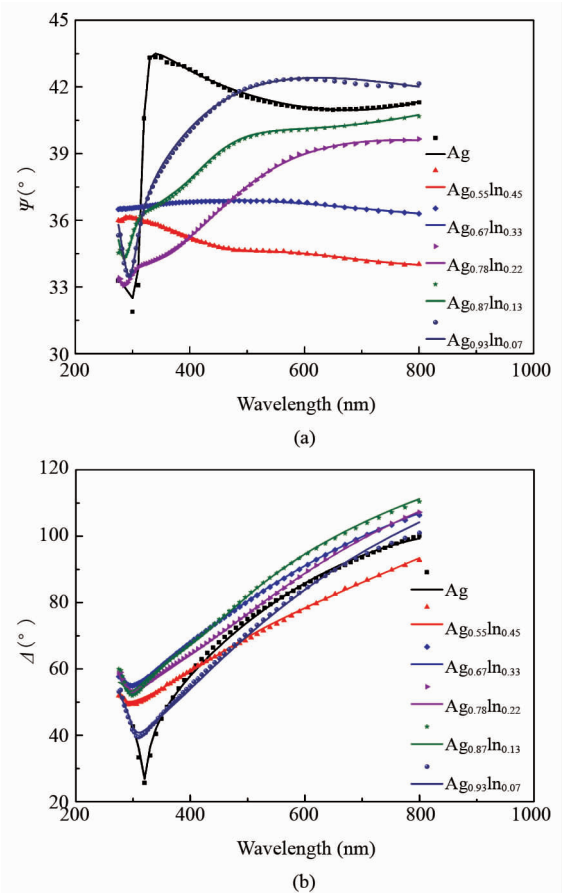

Fig. 2　Experimental data and fitted simulations of the (a) Ψ and (b) Δ of Ag-In alloy films
图 2　银铟合金薄膜椭偏参数(a) Ψ 和(b) Δ 的测得值与拟合值

In the low-energy region of approximately 1.5 ~ 2.5 eV, the Drude formation[24] fits well with the dielectric function of metals, yielding the equation

$$\varepsilon = \varepsilon_\infty - \frac{\omega_p^2}{\omega^2} + i\frac{\omega_p^2}{\omega^3\tau}, \quad (3)$$

where τ is the relaxation time of electrons. An empirical formula[25] can be applied, and τ is expressed by

$$\frac{1}{\tau} = \frac{1}{\tau_0} + \beta\omega^2. \quad (4)$$

For noble metals, β originates from electron-electron scattering, electron-phonon scattering, and electron-impurity scattering[26]. The values of the parameters $1/\tau_0$ and β (Fig. 4) increase with increasing In concentrations in the alloy films, leading to higher scattering frequencies, which result in large damping and great energy loss. The results agree well with those of ε_2.

Quality (Q) factors are used to evaluate the performance of various plasmonic materials[11], including lo-

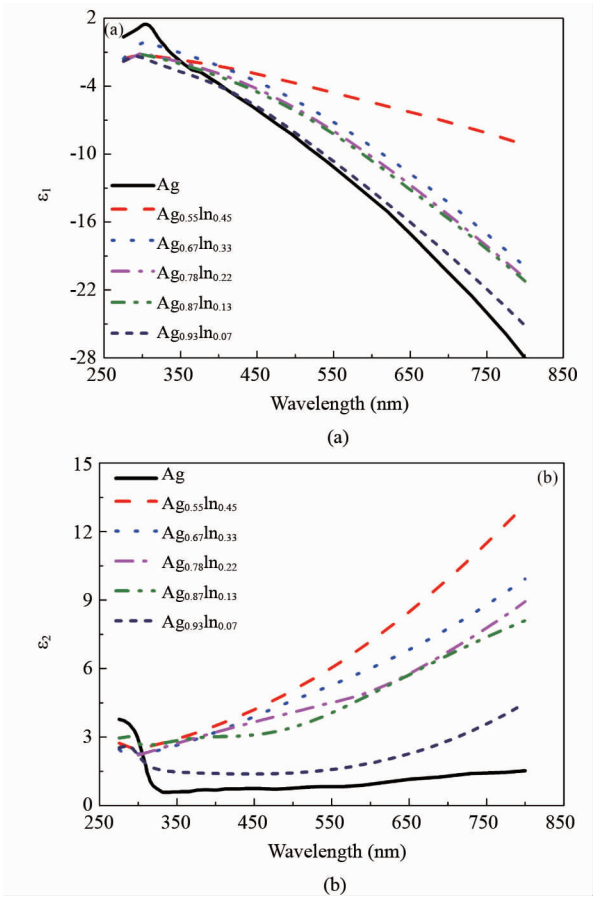

Fig. 3 Dielectric function spectra of Ag-In alloy films
图3 银铟合金薄膜的介电函数谱

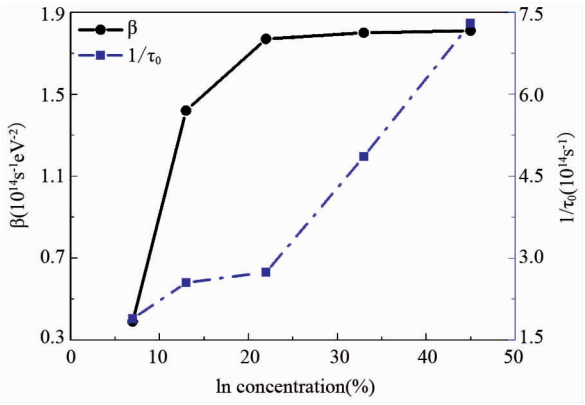

Fig. 4 Dependence of β and $1/\tau_0$ on In concentration
图4 β 和 $1/\tau_0$ 随铟含量的变化

cal surface plasmons ($Q_{lsp} = -\varepsilon_1/\varepsilon_2$) and surface plasmon polaritons ($Q_{spp} = -\varepsilon_2/\varepsilon_2$). Figure 5 displays the Q factors of the alloy films with different compositions, showing that the magnitudes of the Q factors decline with increasing In concentration in the alloy films. The $Ag_{0.93}In_{0.07}$ alloy film exhibits Q factors that exceed those of pure Au and Cu in certain frequency ranges[23]. The addition of In in Ag-In alloys was shown to be capable of modulating the alloys' electronic band structure, improving the optical properties and performance of plasmonic materials. This modulating effect suggests that Ag-In alloys are promising plasmonic materials for potential application in multiple fields.

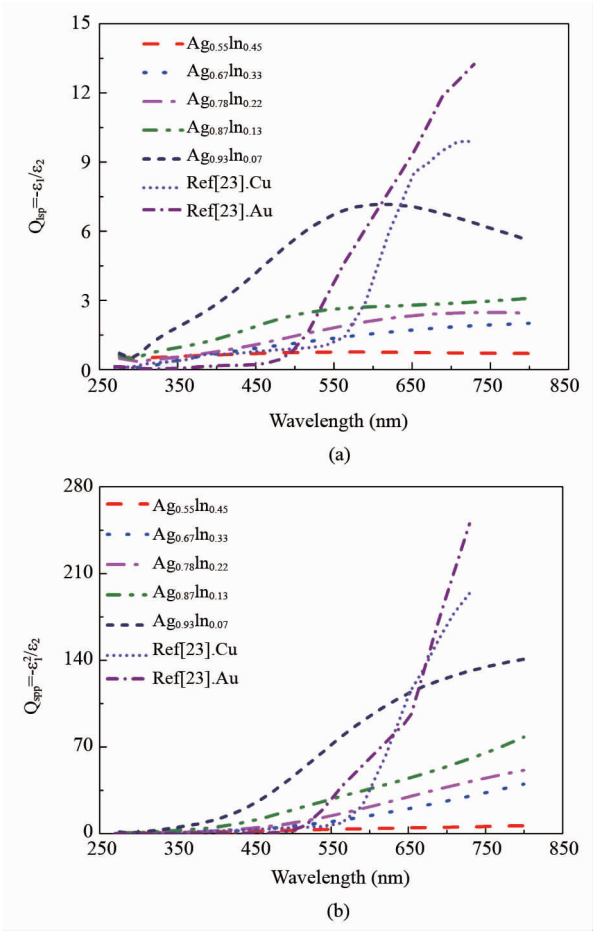

Fig. 5 Q factors of alloy films with different compositions, as well as those of pure Cu and Au
图5 不同组分银铟合金薄膜以及铜和金的品质因子

Figure 6 reveals the energy-loss function (ELF) of Ag-In alloy films. The ELF is given by the imaginary component of the inverse of the dielectric constant,

$$-\mathrm{Im}(\tilde{\varepsilon}^{-1}) = \frac{\varepsilon_2}{\varepsilon_1^2 + \varepsilon_2^2} \quad . \quad (5)$$

This quantity measures the probability that a normal incident charged particle will excite a long-wavelength plasmon, and hence induce an energy loss equal to the energy of the plasmon[27]. In Fig. 6, the ELFs of all films display typical peaks at around 300 nm; the peak intensities decrease with increasing In concentrations, but the peaks broaden and shift toward shorter wavelengths (blue-shifting). The peak height of the ELF is measured by $1/\varepsilon_2$. ε_2 is increased by the three processes of increasing τ of free carriers, broadening the strong L_3-$L_2'(E_F)$ transition, where E_F represents the Fermi energy, and shifting the $L_2'(E_F)$ -L_1 transition to lower energies[28].

The results of the joint density-of-state (JDOS) function for the alloy films are shown in Fig. 7. The JDOS values of the alloy films clearly increased with in-

creasing In concentrations in the long-wavelength range[29-30], illustrating the stronger interband transitions in the alloy films with larger In components, which also accounted for the increase in ε_2.

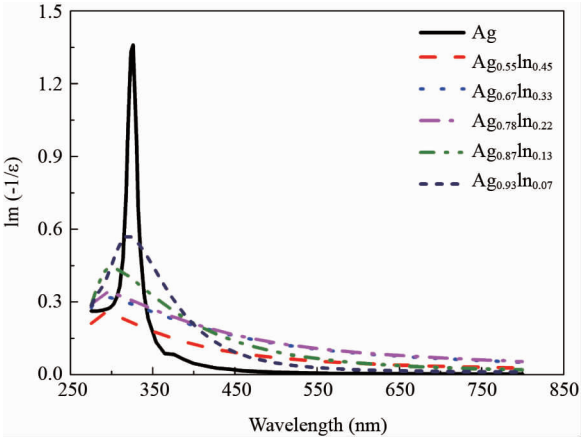

Fig. 6　Energy loss spectra of Ag-In alloy films
图 6　银铟合金薄膜的能量损失谱

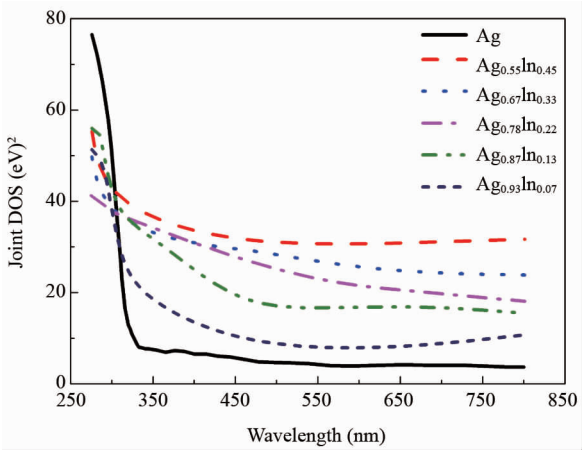

Fig. 7　Joint density-of-state values for deposited Ag-In alloy films
图 7　银铟合金薄膜的联合态密度

3　Conclusion

This study investigated the optical properties of Ag-In alloys with different compositions deposited by magnetron sputtering, on Si substrates. A typical interband transition peak of the alloy films located above 4.0 eV is observed to blue-shift from its original value in pure Ag, according to the change in ε_2. The dielectric function spectra of these films show that the optical properties are sensitive to In concentrations in the Ag-In alloys. The added In causes variations in the electronic band structure, which ultimately lead to changes in the alloys' optical properties. The quality factors Q_{lsp} and Q_{spp} both decrease with increasing In content, and the $Ag_{0.93}In_{0.07}$ alloy film has Q factors exceeding those of pure Au and Cu in a certain wavelength range. By adjusting In concentration to minimize the energy loss of the alloy components, the resulting Ag-In alloys have the potential for application in metamaterials and plasmonic devices.

Acknowledgement

This work was supported by the NSFC (Grant No. 61275160, 11374055, 11174058, 60938004), the STCSM project of China (Grant No. 12XD1420600).

References

[1] Alu A, Engheta N. Plasmonic and metamaterial cloaking: physical mechanisms and potentials[J]. *Journal of Optics A: Pure and Applied Optics*, 2008, **10**: 093002.
[2] Zentgraf T, LIU Yong-Min, Mikkelsen M H, *et al*. Plasmonic Luneburg and Eaton lenses[J]. *Nature Nanotechnology*, 2011, **6**: 151-155.
[3] FU Yong-Qi, ZHOU Xiu-Li. Plasmonic Lenses: A Review[J]. *Plasmonics*, 2010, **5**: 287-310.
[4] Pendry J B. Negative Refraction Makes a Perfect Lens[J]. *Physical Review Letters*, 2000, **85**: 3966-3969.
[5] Blaber M G, Arnold M D, Ford M J. Designing materials for plasmonic systems: the alkali-noble intermetallics[J]. *Journal of Physics: Condensed Matter*, 2010, **22**: 095501.
[6] Boltasseva A, Atwater H A. Low-Loss Plasmonic Metamaterials[J]. *Science*, 2011, **331**: 290.
[7] Noginov M A, Zhu G, Bahoura M, *et al*. The effect of gain and absorption on surface plasmons in metal nanoparticles[J]. *Applied Physics B: Lasers and Optics*, 2007, **86**: 455-460.
[8] Noginov M A, Podolskiy V A, Zhu G, *et al*. Compensation of loss in propagating surface plasmon polariton by gain in adjacent dielectric medium[J]. *Optics Express*, 2008, **16**: 1385-1392.
[9] Khurgin J B, Sun G. In search of the elusive lossless metal[J]. *Applied Physics Letters*, 2010, **96**: 181102.
[10] Thylén L, Holmström P, Bratkovsky A, *et al*. Limits on Integration as Determined by Power Dissipation and Signal-to-Noise Ratio in Loss-Compensated Photonic Integrated Circuits Based on Metal/Quantum-Dot Materials[J]. *IEEE Journal of Quantum Electronics*, 2010, **46**(4): 518-524.
[11] West P R, Ishii S, Naik G V, *et al*. Searching for better plasmonic materials[J]. *Laser Photonics Review*, 2010, **4**: 795.
[12] Rivory J. Comparative study of the electronic structure of noble-metal-noble-metal alloys by optical spectroscopic[J]. *Physical Review B*, 1977, **15**(6): 3119-3135.
[13] SONG Jin-Tao, LI He-Yin, LI Jing, *et al*. Fabrication and optical properties of metastable Cu-Ag alloys[J]. *Applied Optics*, 2002, **41**: 5413.
[14] Morgan R M, Lynch D W. Optical Properties of Dilute Ag-In Alloys[J]. *Physical Review*, 1968, **172**(3): 628-640.
[15] Wronkowska A A, Wronkowski A, Bukaluk A, *et al*. Structural analysis of In/Ag, In/Cu and In/Pd thin films on tungsten by ellipsometric, XRD and AES methods[J]. *Applied Surface Science*, 2008, **254**: 4401-4407.
[16] May R A, Kondrachova L, Hahn B P, *et al*. Optical Constants of Electrodeposited Mixed Molybdenum-Tungsten Oxide Films Determined by Variable-Angle Spectroscopic Ellipsometry[J]. *The Journal of Chemical Physics C*, 2007, **111**: 18251-18257.
[17] Tompkins H G, Mcgahan W A. *Spectroscopic Ellipsometry and Reflectometry: A User's Guide*[M], New York: Wiley Inter-Science, 1999.
[18] CHEN Liang-Yao, FENG Xing-Wei, SU Yi, *et al*. Design of a scanning ellipsometer by synchronous rotation of the polarizer and analyzer[J]. *Applied Optics*, 1994, **33**(7): 1299-1305.
[19] Barron L W, Neidrich J, Kurinec S K. Optical, electrical and structural properties of sputtered aluminum alloy thin films with copper, titanium and chromium additions[J]. *Thin Solid Films*, 2007, **515**: 3363.

(下转第 14 页)

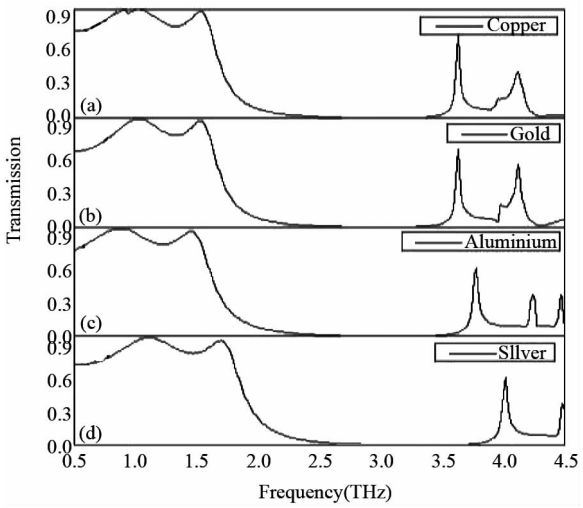

Fig. 6 Simulated transmission spectra of different metal layer with $n=2$

图6 不同种类金属层的模拟透射谱(以 $n=2$ 为例)

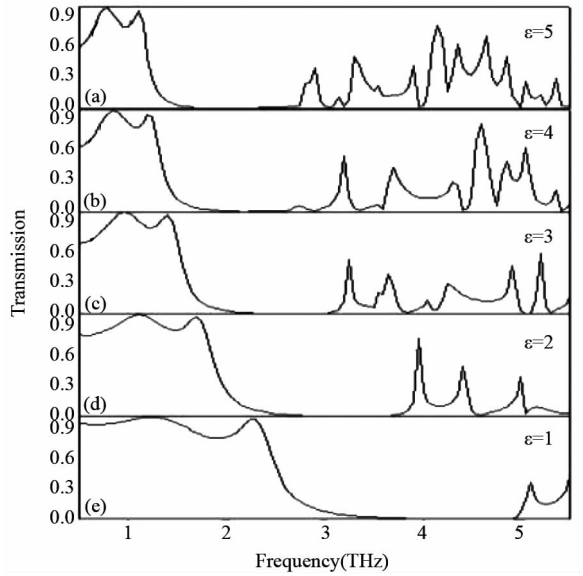

Fig. 7 Simulated transmission spectra of different dielectric constant with $n=2$

图7 不同种类介质层的模拟透射谱(以 $n=2$ 为例)

structure in the THz regime is designed and simulated. Results indicate that a broad stop-band filter is realized through using a multilayer structure consisting of alternating metal layers and dielectric layers. The plasmonic hybridization of inward coupling mode and adjacent unit cells coupling resonance mode leads to the stop-band broader. The stop-bandwidth can reach to 2.2THz with increasing the metal layer number. The stop-band filter is sensitive to the dielectric layer but insensitive to the metal layer. Moreover, the central frequency of stop-band is blue-shifted with n increasing or the dielectric constant of dielectric layer decreasing. A broad stop-band filter can be developed by selecting the appropriate structural parameters, and stacking CRR structure metal layers and dielectric layers.

References

[1] Alaee R, Farhat M, Rockstuhl C, *et al.* A perfect absorber made of a grapheme micro-ribbon metamaterial [J], *Optics Express.*, 2012, **20**: 28017-28024.

[2] Fang N, Lee H. Sun, C, *et al.* Sub-Diffraction-Limited Optical Imaging with a Silver Superlens [J], *Science.*, 2005, **308**:534-537.

[3] LIU Xu, Starr T. Starr A. F, *et al.* Phys. Rev. Lett. 2010, **104**: 207403-207407.

[4] Schuring D, Mock J J, Justice B J, *et al*, Metamaterial Electromagnetic Cloak at Microwave Frequencies [J], Science., vol. 314, pp. 977-981, 2006.

[5] LIU Na, Mesch M, Weiss T, *et al. NanoLett.* 2010, **10**: 2342-2348.

[6] Engheta N, Al'u A, *Filters and feedbacks in metamaterial nanocircuits, presented at the Photonic Metamaterials: From Random to Periodic* [M], Jackson Hole, WY, 2007, Paper ThA1.

[7] Chin J Y, Lu M, CUI Tie-Jun, Metamaterial polarizers by electric-field-coupled resonators [J], *Appl. Phys. Lett.*, 2008, **93**:251903-251905.

[8] LI Zhong-Yang, Yujie J. Ding, Broadband stopband filter for terahertz wave based on multi-layer metamaterial microstructure, [C], *Lasers and Electro-Optics (CLEO)*, Conference,2012.

[9] HUA YL, LI Z L, Analytic modal solution to transmission and collimation of light by one-dimensional nanostructured subwavelength metallic slits [J], *J. Appl. Phys.* 2009, **105**: 013104-013111.

[10] Smith D R, Vier D C, Konschny T, *et al.* Electromagnetic parameter retrieval from inhomogeneous metamaterials[J], *Phys. Rev. E*, 2005, **71**:036617-036627.

[11] Smith D R, Schultz S, Markos P, *et al.* Determination of effective permittivity and permeability of metamaterials from reflection and transmission coefficients[J], *Phys. Rev. B.*, 2002, **65**:195104-195108.

[12] Han N R, Chen Z C, Lim C S, *et al.* Broadband multi-layer terahertz metamaterials fabrication and characterization on flexible substrates [J], *Opt. Exp*, 2011, **19**:6990-6998.

(上接5页)

[20] Woltgens H, Friedrich I, Njorog W K, *et al.* Optical electrical and structural properties of Al-Ti and Al-Cr thin films [J]. *Thin Solid Films*, 2001, **388**: 237-244.

[21] Mookerji B, Stratman M, Wall M, *et al.* The optical constants of gallium stabilized δ-plutonium metal between 0.7 and 4.3 eV measured by spectroscopic ellipsometry using a double-windowed experimental chamber[J]. *Journal of Alloys and Compounds*, 2007, **444**: 339-341.

[22] Pells G P, Montgomery H. The optical properties of α-phase Cu-Zn, Cu-Ga, Cu-Ge and Cu-As alloys [J]. *Metal Physics Supplement*, 1970, **3**: s330.

[23] Palik E D. *Handbook of Optical Constants of Solids*[M]. Orlando: Academic Press, 1985.

[24] Wooten F. *Optical Properties of Solids*[M]. New York: Academic Press, 1972.

[25] Allen J W, Lucovsky G, Mikkelsen J C. Optical properties and electronic structure of crossroads material MnTe[J]. *Solid State Communications*, 1977, **24**(5): 367-370.

[26] Smith J B, Ehrenreich H. Frequency dependence of the optical relaxation time in metals[J]. *Physical Review B*, 1982, 25(2): 923.

[27] Thompson B V. Neutron Scattering by an Anharmonic Crystal [J]. *Physical Review*, 1963, **131**(4): 1420.

[28] Kim K J, Chen L Y, Lynch D W. Ellipsometric study of optical transitions in $Ag_{1-x}In_x$ alloys[J]. *Physical Review B*, 1988, **38**(18): 13107.

[29] O'Learya S K. An analytical density of states and joint density of states analysis of amorphous semiconductors[J]. *Journal of Applied Physics*, 2004, **96**(7): 3680.

[30] Liang W Y, Beal A R. A study of the optical joint density-of-states function[J]. *Solid State Physics*, 1976, **9**: 2824-2833.